

2005

## Throughput and Delay Optimization in WDM FDDI optical Network

Muhsen Aljada  
*Edith Cowan University*

Kamal Alameh  
*Edith Cowan University*

Khalid Al-Begain

Follow this and additional works at: <https://ro.ecu.edu.au/ecuworks>



Part of the [Engineering Commons](#)

---

This is an Author's Accepted Manuscript of: Aljada, M. , Alameh, K. , & Al-Begain, K. (2005). Throughput and Delay Optimization in WDM FDDI optical Network. Proceedings of IFIP VLSI-SoC 2005. (pp. 283-287). Perth. IFIP (international Federation for Information Processing). Available [here](#).

This Conference Proceeding is posted at Research Online.

<https://ro.ecu.edu.au/ecuworks/2934>

## Throughput and Delay Optimization in WDM FDDI Optical Network

Muhsen Aljada<sup>1</sup>, Kamal E. Alameh<sup>1</sup>, and Khalid Al-Begain<sup>2</sup>

<sup>1</sup>Centre for MicroPhotonic Systems, Electron Science Research Institute, Edith Cowan University, Joondalup, WA, 6027, Australia.

<sup>2</sup>Mobile Computing, Communications and Networking Research Group, School of Computing, University of Glamorgan, Pontypridd (Cardiff), CF37 1DL, Wales, UK.

### Abstract

The rapidly growing Internet traffics are driving the demands for higher transmission capacity and higher processing speed, especially for the backbone networks. To support such bandwidth usage an optical Fiber Distributed Data Interface Wavelength Division Multiplexed (FDDI/WDM) network is proposed, wherein the wavelength channels are amplified using Erbium-Doped Fiber Amplifiers (EDFAs) to compensate for the losses over the optical fiber span. In this paper we investigate the network performance for both asynchronous and synchronous transmissions, by measuring the amplified spontaneous emission (ASE) along the ring, the optical signal to noise ratio (OSNR), and the electrical SNR at different destinations. The effects of various network parameters such as synchronous bandwidth allocation and Target Token Rotation Time (TTRT) on the network performance are also presented. Results show that when FDDI is used in conjunction with WDM higher throughput and less delay are simultaneously achieved in comparison with FDDI standard networks.

### 1. Introduction

Over the past decade, we have witnessed a rapid growth in optical communication. At first, it was used for long distance links. Currently, optical transmission is finding growing applications in local and metro networks. The transmission bit rate becomes higher and higher, and despite the fact that single mode fiber has a substantial bandwidth, wavelength division multiplexing (WDM) becomes the best choice for capacity increase at lower cost, and its applications extend beyond the optical communications domain [1]. Optical WDM networks are dominating the communication network infrastructure supporting the next generation Internet backbone. However, current applications of WDM focus on the static use of individual WDM channels, which are not exploited efficiently for optimum throughput. The current challenge is to combine the advantages of using WDM in metro optical networks to realize high-throughput optical backbone networks [2]. Current Dense WDM allows 80-120 wavelengths per fiber to be transmitted enabling a total capacity of up to 400 Gb/s

[3]. Fibre Distributed Data Interface (FDDI) is a backbone network defined by American National Standards Institute (ANSI). It uses timed token access method to share the medium among stations, and based on a 100 Mb/s single channel transmission. FDDI networks can have a maximum of 500 nodes connected by using a ring topology, as shown in Fig 1. The maximum allowed length of the medium in the network is 200 km [4].

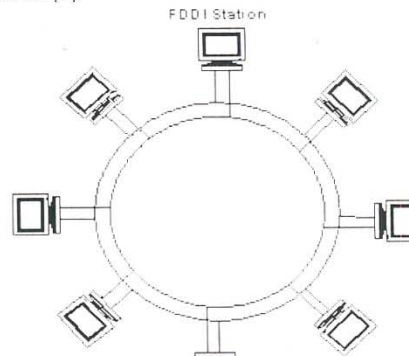


Figure 1. FDDI Network

During network initialization, a parameter called Target Token Rotation Time (TTRT) is assigned for the network together with synchronous bandwidth allocation (which is a fraction of TTRT). There are two modes of transmission in FDDI network: Synchronous and Asynchronous. Time-constrained applications such as voice and real-time traffic use the synchronous mode, whereas applications that do not have time constraints use the asynchronous mode. Synchronous frames are given higher priority over asynchronous frames [5]. When a station receives the token, it starts transmitting its synchronous messages for a time that does not exceed its allocated synchronous time slot. After transmitting a synchronous frame, asynchronous frames can be transmitted for a time interval called the Token Holding Time (THT). The node that captures the token releases must release it immediately either after the THT expires

that can steer an incident optical beam by an angle that depends on the period of the waveform. The far field of an  $m$ -phase-level blazed grating of period  $p$  and aperture  $A$  is given by [7]

$$R(x) = \left[ \text{rect}\left(\frac{x}{p}\right) \varphi(x) \right] * \left[ \sum_{m=1}^N \delta(x - m \cdot p) \cdot \text{rect}\left(\frac{x}{A}\right) \right] \quad (1)$$

where  $*$  denotes convolution,  $\varphi(x)$  is the phase profile of the blazed grating, and  $N$  is the number of period along the blazed grating length. The far field distribution of the blazed grating is given by

$$E = FT[R(x)] \quad (2)$$

where FT denotes the Fourier transform operator. Practically, the diffractive efficiency of the grating generated by the Opto-VLSI processor depends on several factors, namely, (i) linearity of voltage-phase response, (ii) the maximum available phase level, and (iii) the number of quantized phase levels. In general, the overall diffraction efficiency of a blazed grating can be expressed as

$$\eta = \eta_r \cdot \eta_p \cdot \eta_m \quad (3)$$

In Eq. (3),  $\eta_r$  is due to the reflection at the surface of the grating as well as the absorption along the thickness of the grating.  $\eta_p$  is associated with the pixellated nature (defined by the fill factor) of the Opto-VLSI processor, and is given by  $\eta_p = \frac{I_0}{I}$ , with  $I_0$  is the intensity the zeroth-order beam when the Opto-VLSI processor is not addressed, and  $I$  is the input beam intensity.  $\eta_m = \text{Sinc}\left(\frac{\pi}{q}\right)^2$  is related to the number

of quantized phase level,  $q$ , and  $\eta_m$  is linked to the maximum available phase shift. For an ideal blazed grating on which the linear phase-only modulation depth of  $2\pi$  is applied,  $\eta_m$  is equal to 1.

Figure 2 shows the phase profiles for an ideal blazed grating of maximum available phase of  $2\pi$ , together with linear and piecewise-linear blazed gratings of maximum phase level  $k2\pi$ , with  $k < 1$ .

For the linear blazed grating the phase profile can be represented as:

$$\varphi(x) = k \cdot 2\pi \cdot x \quad (4)$$

For the modified blazed grating, the phase profile is given by:

$$\varphi(x) = \begin{cases} 0 & x \leq Z_b \\ k \cdot 2\pi \cdot x & Z_b < x < p - Z_b \\ k \cdot 2\pi & p - Z_b \leq x \leq p \end{cases} \quad (5)$$

Figure 3 shows the theoretical diffraction efficiency of the zero order and first order beam versus the maximum available phase for the linear and piecewise-linear blazed gratings of 32-pixel period when  $Z_b = 0$ ,  $Z_b = 3$ . It is shown that for a maximum available phase

below  $1.8\pi$ , the first-order diffraction efficiency of the piecewise-linear blazed grating is greater than that of the linear blazed grating. For a maximum available phase of  $1.1\pi$ , a 15% improvement in first-order diffraction efficiency is achieved by modifying the linear blazed grating with a piecewise-linear blazed grating.

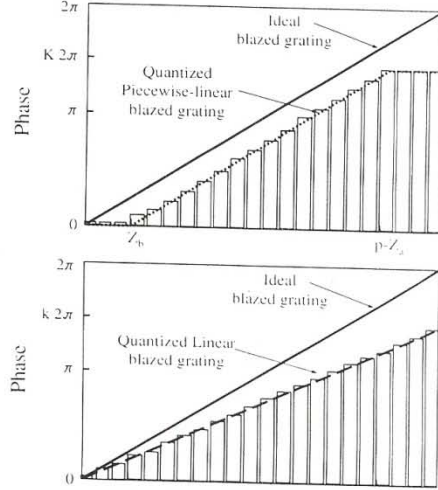


Figure 2. Quantized linear and piecewise-linear blazed gratings with maximum phase less than  $2\pi$ .

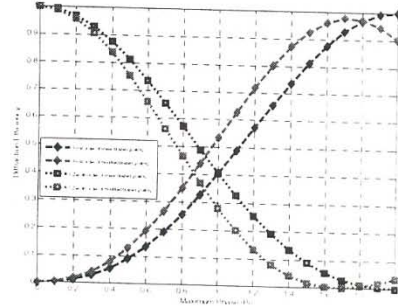


Figure 3. Theoretical diffraction efficiency of 1<sup>st</sup> order and zero order beams versus the maximum phase for linear and piecewise linear blazed gratings of 32-pixel period.

### 3. Experimental Results

The Opto-VLSI processor used in our experiment is a commercially available 1x4096 nematic liquid crystal fabricated by Boulder Nonlinear, Inc. The device consists of 4096 electrode strips that are  $1.0\mu\text{m}$  wide and approximately 6mm long, with a dead-spacing of  $0.8\mu\text{m}$ . The experimental setup is shown in Figure 4. A 1550nm 10dBm optical signal was launched into the input fibre and collimated at 1-mm diameter. Through a beam expander, the beam was expanded to 4-mm in diameter to illuminate the working area of the Opto-

VLSI processor. To measure the diffraction efficiency, the diffracted beam was focused through an imaging lens on the photodetector of a free-space power meter. The input fibre collimator, the imaging lens and photodetector were placed on 5-axis stages so that they can be accurately aligned with respect to each other. The measured optical loss introduced by Opto-VLSI processor was around 3dB, which was due to low mirror reflectivity and low fill factor. A polarization controller was also used to reduce the polarization dependent loss.

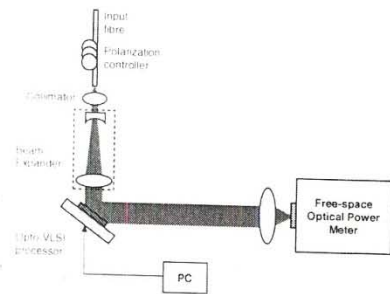


Figure 4. Experimental setup for measuring the diffraction efficiency of blazed gratings.

Figure 5 shows the measured normalized diffraction efficiency of the first order beam for the linear blazed grating and the piecewise-linear blazed grating. When the maximum available phase is greater than  $1.8\pi$ , the linear blazed grating has higher diffraction efficiency. However, for a maximum available phase less than  $1.8\pi$ , the piecewise-linear blazed grating can attain substantially higher diffraction efficiencies than the linear blazed grating. For example, for a maximum available phase of  $1.2\pi$ , the diffraction efficiency of a piecewise linear grating of 32-pixel period is more than 70%, whereas the diffraction efficiency of a similar period linear blazed grating is less than 45%.

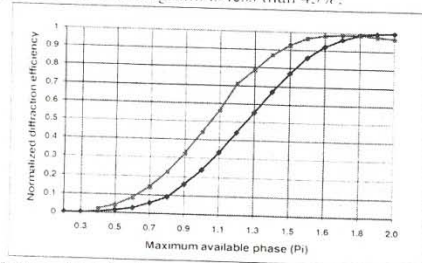


Figure 5. Normalized measured diffraction efficiency versus the maximum available phase for the linear (diamond) and piecewise linear (square) blazed gratings ( $Z_0=0$ ,  $Z_1=3$ ).

#### 4. Conclusions

In this paper, the degradation in diffraction efficiency due to the voltage drop across the quarter wave plate layer of an Opto-VLSI processor has been investigated, and the use of piecewise-linear blazed gratings, rather

than conventional linear blazed gratings, for beam steering is proposed to improve the diffraction efficiency of Opto-VLSI processors. We have analysed and measured the diffraction efficiencies of linear and piecewise-linear blazed gratings generated by an Opto-VLSI processor having a maximum available phase of less than  $2\pi$ . Experimental results have shown that piecewise-linear blazed gratings can attain higher diffraction efficiencies than linear blazed gratings when the maximum available phase is limited to less than  $1.8\pi$ . For an Opto-VLSI processor having a maximum available phase of  $1.2\pi$ , a diffraction efficiency of more than 70% can be attained with a piecewise-linear blazed grating, in comparison to 45% efficiency for a conventional linear blazed grating.

#### 5. Acknowledgement

This project is support by Australian Research Council (ARC) and the Office of Science and Innovation, Western Australian Government.

#### Reference:

- [1] M. Raisi, S. Adherom, K. Alameh and K. Eshraghian, "Opto-VLSI-based multiband tunable optical filter", *IEEE Electron. Lett.*, vol. 39, No. 21, pp. 1533-1534, 2003.
- [2] S. Adherom, M. Raisi, K. Alameh and K. Eshraghian, "Adaptive WDM equalizer using Opto-VLSI beam processing", *IEEE Photonics Technology Letters*, Vol.15, no.11, pp.1603-1605, Nov.2003.
- [3] Pedro M. Prieto, Enrique J. Fernández, Silvestre Manzanera, Pablo Artal, "Adaptive optics with a programmable phase modulator: applications in the human eye", *Optics Express*, Vol. 12, No. 17, August 2004, pp. 4059-4071.
- [4] M. Komarcevic, I. G. Manolis, T. D. Wilkinson, and W. A. Crossland, "Polarization effects in reconfigurable liquid crystal phase holograms," *Opt. Commun.*, vol. 244, pp. 105-110, 2005.
- [5] W. Singer and H. Tiziani, "Born approximation for the nonparaxial scalar treatment of thick phase gratings," *Appl. Opt.* **37**, pp. 1249-1555, 1998.
- [6] U. Levy, E. Marom, and D. Mendlovic, "Thin element approximation for the analysis of blazed gratings, simplified model and validity limits," *Opt. Commun.* **229**, 11-21, 2004.
- [7] X. Wang, D. Wilson, R. Muller, P. Maker, and D. Psaltis, "Liquid-crystal blazed-grating beam deflector," *Appl. Opt.* **39**, 6545-6555, 2000.
- [8] E. G. Loewen, M. Nevière, and D. Maystre, "Grating efficiency theory as it applies to blazed and holographic gratings," *Appl. Opt.* **16**, 2711-2721, 1977.